

# Comparison of Molecular Dynamics and Monte Carlo Computer Simulations of Spinodal Decomposition

S. W. Koch<sup>1,2</sup> and Rainer Liebmann<sup>1</sup>

*Received March 8, 1983; revised April 22, 1983*

---

The main results of recent computer simulations of spinodal decomposition in various systems are summarized and compared. Both Monte Carlo simulations of the kinetic Ising system and molecular dynamics simulations of phase separation in Lennard-Jones systems yield power law growth for the coarsening of the decomposition pattern and scaling of the spinodal peak of the structure factor. These similarities and also distinct differences of the dynamics of one- and two-component systems and of the different simulation techniques are discussed.

---

**KEY WORDS:** Phase separation; computer simulation techniques; scaling; cluster growth laws.

## 1. INTRODUCTION

Spinodal decomposition is the decay process of spatially homogeneous states in the unstable part of the phase diagram of certain systems. The dynamics of the decomposition process displays a variety of physically interesting features such as different growth regimes of the formed clusters and scaling behavior of the pertinent structure factor.

Experimentally, spinodal decomposition is mostly studied in binary systems,<sup>(1)</sup> such as binary alloys<sup>(2)</sup> or fluids,<sup>(3)</sup> which have been quenched into the miscibility gap of their phase diagram. The relevant time scale for the phase separation process is on the order of fractions of seconds in binary liquids and on the order of minutes or even many hours in metallic

---

<sup>1</sup> Institut für Theoretische Physik der Universität Frankfurt, Robert-Mayer-Strasse 8, D-6000 Frankfurt-Main, Federal Republic of Germany.

<sup>2</sup> IBM Research Laboratory, San Jose, California, USA.

alloys. The theoretical description is successfully given in the framework of the generalized diffusion equation of the Cahn–Cook theory, important contributions coming, e.g., from Langer and coworkers.<sup>(1)</sup> A somewhat more general ansatz is due to Binder and coworkers,<sup>(4)</sup> who treat spinodal decomposition within a nucleation theory. A recent summary of spinodal decomposition in binary systems is given in Ref. 5.

Reasonably different is the situation for one-component systems, such as a van der Waals-like liquid quenched below the critical point into the unstable region of its liquid–gas phase diagram. Spinodal decomposition in this system takes place within several picoseconds; a diffusion equation is no adequate description, and instead one may, e.g., treat the equations of fluctuating hydrodynamics.<sup>(6)</sup> Because of the short times involved, no laboratory experiments on these systems are available yet.

But, besides the laboratory experiments, there is another increasingly important source of physical information concerning phase-separating and other physical systems. These are studies by numerical simulations of the involved dynamical processes. Two major techniques are used in this context, the Monte Carlo simulation technique and molecular dynamics simulations.

It is our aim in this paper to summarize the special features of Monte Carlo<sup>(7)</sup> and molecular dynamics simulations<sup>(8)</sup> of spinodal decomposition. To a certain extent it appears, as if both dynamically quite different techniques would yield similar results for the different physical systems concerning, e.g., simple power laws for the growth of the pertinent decomposition patterns and scaling relations for the spinodal peak of the time-dependent structure factor, or equivalently of the cluster part of the radial distribution function.

We will summarize the results of molecular dynamics simulations of the one-component system in Section 2 and those of the Monte Carlo simulations of the kinetic Ising model in Section 3 of this paper. In Section 4 we analyze and discuss the obtained results.

## 2. MOLECULAR DYNAMICS SIMULATIONS

The molecular dynamics (MD) simulation technique is the direct numerical integration of Newton's equations of motion for a given number of particles. These particles are free to move in a specified cell according to their mutual interactions. Details of the numerical method are described in Refs. 9 and will not be repeated here.

Molecular dynamics simulations are best suited for the direct investigation of time-dependent processes since they yield the numerically correct

time evolution of the complete system. For long-time studies of large systems (i.e., several thousand particles) one needs highly precise fast integration routines, which are available but nevertheless require a quite considerable amount of computer time. This may be one of the reasons why relatively few molecular dynamics simulations for phase separation processes in physical systems have been reported so far. However, recently molecular dynamics simulations have been performed to study spinodal decomposition in a one-component Lennard–Jones system, in which the atoms were free to move in three<sup>(10)</sup> or in two dimensions.<sup>(8)</sup>

Since the results of the simulation of the two-dimensional system are by far more complete than those of the three-dimensional one and since furthermore most of the essential results are independent of dimensionality, we restrict ourselves for the purpose of this paper to a brief summary of the results for the two-dimensional system (see Ref. 8 for the details). These results have been obtained in various simulations for atoms interacting by a Lennard–Jones potential

$$\varphi(r) = 4\epsilon \left\{ \left( \frac{\sigma}{r} \right)^{12} - \left( \frac{\sigma}{r} \right)^6 \right\},$$

where  $r$  is the interatomic separation and  $\epsilon, \sigma$  are the Lennard–Jones parameters. One can divide the molecular dynamics computer experiments of Ref. 8 into two categories according to which thermodynamic parameters have been fixed during the respective simulation. In all cases the atomic density was constant corresponding to the value of the critical density for liquid–vapor coexistence in Lennard–Jones systems. Additionally, in some of the simulations the atomic velocity distribution was renormalized every time-step in order to fix the average system temperature to a given value below the critical temperature. These are the constant temperature simulations. If the velocity renormalization is not performed, appropriate solution of Newton’s equations requires time independence of the total energy, i.e., one performs constant energy simulations. In both kinds of molecular dynamics simulations spinodal decomposition has been observed. In the left-hand column of our Fig. 1, we reproduce for later comparison to Monte Carlo results some of the snapshot pictures of Ref. 8. These pictures show the atomic configurations for the constant temperature simulation at the times which are indicated at the respective figures. In Ref. 8, a detailed analysis of the numerical data has been reported and it has been concluded that in all simulated situations the observed phase separation process could be divided into two main time regimes, the first of which was completed as soon as the local density extremes reached the respective values of the gas and liquid density. The second time regime was still not completed as the simulations were stopped. For this regime, growth laws for

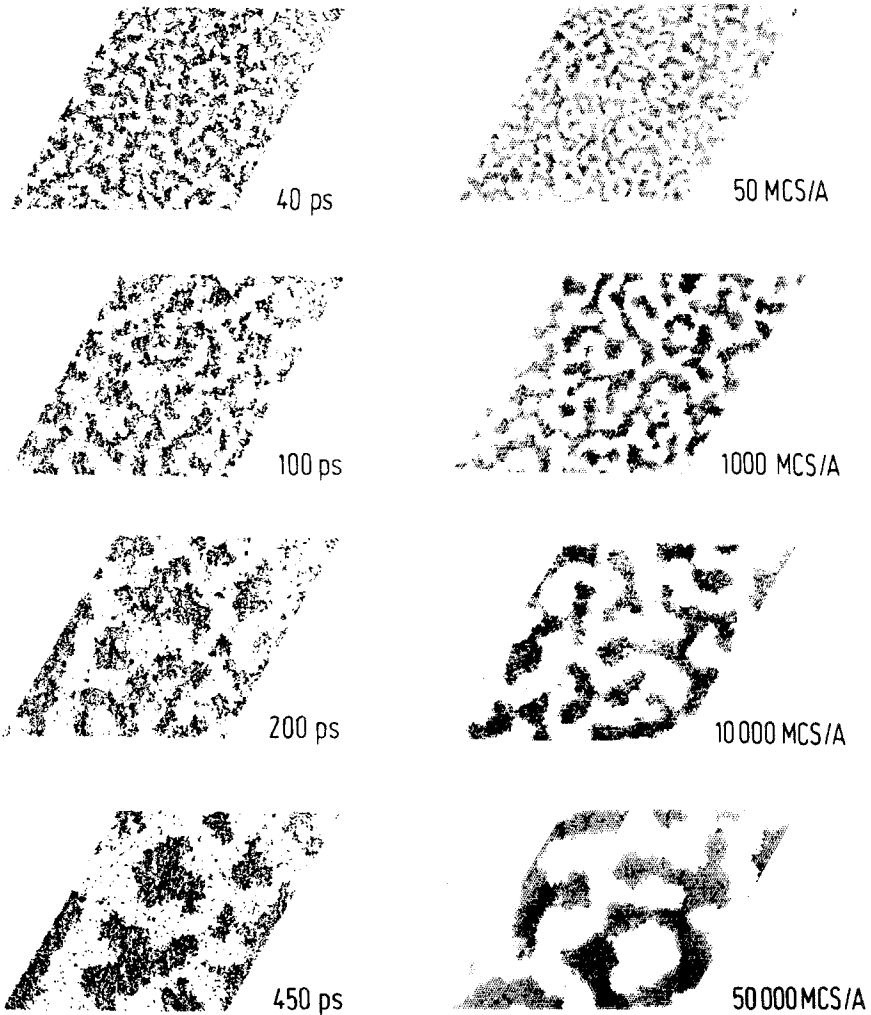


Fig. 1. Snapshots of the cluster growths pattern obtained from molecular dynamics (left column) and Monte Carlo version I (right column). Each pair of snapshots is chosen to have equal mean cluster radius  $R$ .

the average cluster size  $R(t)$  have been obtained and shown to be in agreement with theoretical predictions. For the details of the calculation compare Ref. 8. Particularly it was shown, that  $R(t) \propto t^{1/2}$  for the constant temperature and  $R(t) \propto t^{1/3}$  for the constant energy simulations. The theoretical analysis<sup>(8)</sup> shows that these growth laws are the same in two and three dimensions.

Additionally, a coarse-grained scaled radial distribution function could be obtained by the relation

$$G(X) = g(X, t), \quad X = r/R(t)$$

Here,  $g(r, t)$  is the cluster radial distribution function which was calculated from the full distribution function by averaging over radial intervals greater than the period characteristic of the atomic short-range order. The Fourier transform of  $g(r, t)$  yields the spinodal peak of the time-dependent structure factor  $S(k, t)$ . In Ref. 8 it was demonstrated that  $g(x, t)$  is time invariant within the above-mentioned growth regimes in the phase separation process.

Thus, in the molecular dynamics simulations<sup>(8)</sup> two results have been obtained (besides others not mentioned here): (i) the growth law dynamics of the average cluster size and (ii) scaling of the cluster radial distribution function, i.e., of the Fourier transform of the spinodal peak of the time-dependent structure factor.

### 3. MONTE CARLO SIMULATIONS

Monte Carlo (MC) techniques are by now a standard method to investigate properties of systems in thermodynamic equilibrium. For a review see, e.g., the book by Binder.<sup>(11)</sup> In this paper we are interested in applications of MC methods to determine dynamical features of phase-separating systems. We therefore discuss briefly the stochastic nature of the time evolution of MC systems.

In MC simulations successive configurations of a simulated many-particle system are generated by changing the positions of usually one or two particles according to the probability  $W(x_v \rightarrow x_v')$ . The probability for such a move depends on the pertinent change of the energy

$$\Delta E = E_{v'} - E_v$$

where  $E_v$  symbolizes the energy of the system with the configuration  $x_v$ .  $W$  is chosen such that time averages over successive configurations converge to the correct thermodynamic equilibrium values. However, this requirement does not determine  $W$  uniquely. Two commonly used choices are

$$W(x_v \rightarrow x_v') \propto e^{-\beta\Delta E} / (1 + e^{-\beta\Delta E}) \quad (a)$$

and

$$W(x_v \rightarrow x_v') \propto \begin{cases} e^{-\beta\Delta E}, & \Delta E > 0 \\ 1, & \text{otherwise} \end{cases} \quad (b)$$

The intrinsically stochastic dynamics of the MC method is the reason why the sequence of generated configurations does in general not correspond to

a true physical time evolution, when the latter is governed by deterministic kinetic equations.<sup>(12)</sup> On the other hand, there are physical systems in which the MC kinetics may be assumed to mimic correctly the true time evolution. An example is the process of spinodal decomposition in binary alloys under the assumption that the pairwise exchange of nearest-neighbor (nn) atoms dominates the kinetic properties. In this particular case the binary alloy problem maps onto the kinetic Ising system with Kawasaki dynamics.<sup>(7)</sup> MC simulations for this system have been performed by Lebowitz and coworkers and the results have been presented in a series of papers.<sup>(7)</sup> One of the main results is the dynamic scaling of the time-dependent structure factor  $S(k, \tau)$  in the late-time regimes of the various simulations

$$S(k, \tau) \propto K^{-d}(\tau) \cdot F[k/K(\tau)]$$

with

$$K(\tau) \propto \tau^{-a}$$

Here, the constant  $a$  depends on the temperature and on the concentrations  $c_A$  and  $c_B$  of  $A$  and  $B$  atoms in the binary alloy. Note that  $\tau$  is the MC analog of time in units of MC steps/atoms (MCS/A). For later comparison we quote the values of the simulations for a system with simple cubic lattice:

$$a = 0.25 \quad \text{for} \quad T/T_c = 0.59 \quad \text{and} \quad c_A = 0.5 = c_B$$

( $a$  is supposed to be independent of the dimensionality  $d$  of the simulated system).

In order to compare more directly the results of MC simulations with those obtained using the molecular dynamics method described in the previous section, we performed a series of MC simulations for the dynamics of spinodal decomposition of a lattice gas system, which simply can be mapped on the equivalent binary alloy by regarding occupied/vacant sites as A/B atoms.

We studied a system of  $99 \times 99$  lattice sites on a triangular lattice and a particle concentration  $c = 0.45$ , i.e., we simulated the motion of 4410 atoms with periodic boundary conditions. The concentration of 0.45 gives approximately the same ratio of fluid-to-gas phases as in the MD snapshots (left column of Fig. 1) and is slightly below the site percolation threshold of 0.50 for this lattice. For the transition probability  $W$  we chose the form (b) and assumed nn interactions, contrary to the MD simulations, but as in the alloy system.

We tested three MC versions differing only in the vacant sites available for the randomly chosen particle to be displaced: (I) only nearest-neighbor vacancies available, (II) all vacancies available with the same

probability, (III) straight “flight” in one of the six nearest-neighbor directions until stopped by the next particle on this path.

Version (I) is identical to the MC kinetics used in the binary alloy problem.<sup>(7)</sup> Version (II) has been used, e.g., by Leamy, Gilmer, and Jackson<sup>(13)</sup> to study the static properties of the liquid–gas interface in the Ising model. Version (III) should not be taken too seriously, since it does not reproduce the correct static properties due to the correlations built in by the condition “until stopped . . .” It is only included as an extreme case for the comparison of different MC dynamics.

For our simulations we always used completely random start configurations corresponding to  $T = \infty$  and performed quenches to the fixed temperature  $T/T_c = 0.60$ . We analyzed the data in the same way as the molecular dynamics simulation summarized in the previous section. Especially, we have calculated the coarse-grained radial distribution function  $g(r, \tau)$  which allows to define a mean cluster radius  $R(\tau)$ .<sup>(8)</sup>

MC snapshot pictures from version I are shown in the right column of Fig. 1 and show cluster patterns quite similar to the MD snapshots of the left column.

The evolution of  $R(\tau)$  for all three MC versions is plotted in Fig. 2 on a double logarithmic scale. MC version I yields two different growth

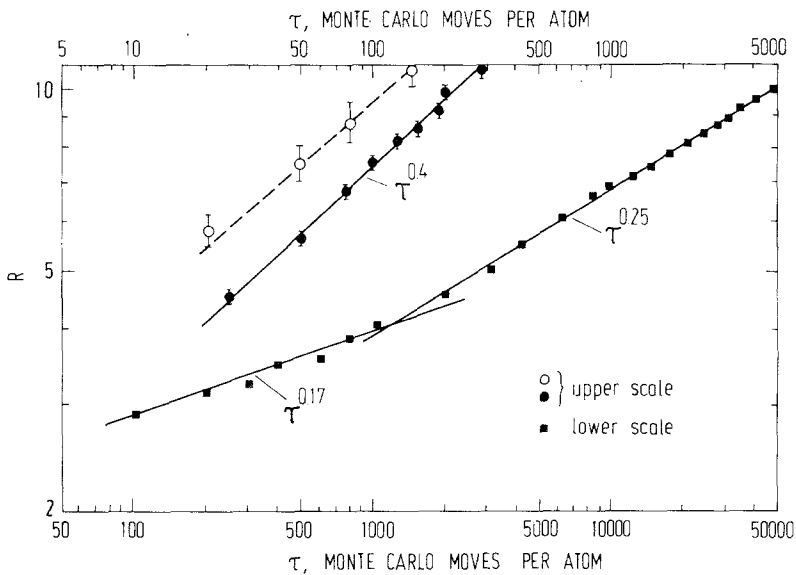


Fig. 2. Mean cluster radius  $R$  versus Monte Carlo time  $\tau$  (in MCS/A) for the three MC versions (MC version I: squares, MC version II: open circles, MC version III: full circles. For details see text). Note the shift between lower and upper time scale.

regimes. In the first one ( $\tau < 10^4$  MCS/A, lower scale)  $g(r, \tau)$  does not scale, whereas good scaling is found in the later part of the second regime  $5 \times 10^4 < \tau < 6 \times 10^5$  MCS/A. The upper limit is caused by finite size effects due to the limited number of simulated particles. In the second regime  $R(\tau) \propto \tau^{a_I}$  with  $a_I = 0.25 \pm 0.01$ . These results are in good agreement with the findings for the binary alloy problem<sup>(7)</sup> on the square and simple cubic lattice. (For  $T/T_c = 0.8$  we also determined the growth law which was identical to the reported results for  $T/T_c = 0.6$ .) Different random start configurations caused only very small changes in the detailed behavior of  $g(r, \tau)$ .

For the MC version II, where the particles can jump into any vacancy in the system, the usual spatial oscillations in  $g(r, \tau)$  are considerably reduced compared, e.g., to the results of MC version I. Especially for short times the first minimum in  $g$ , characterizing the depletion zone around clusters,<sup>(8)</sup> is very shallow and the obtained  $R(\tau)$  differs considerably for different random start configurations. We observe no scaling behavior. A power law fit for  $R(\tau)$  yields an exponent  $a_{II} = 0.38 \pm 0.08$ . This is much larger than  $a_I$  due to the faster cluster growth.

Finally, for MC version III, where the particles travel straight until they hit another one, the shape of  $g$  resembles the results of version I. Scaling is fulfilled approximately and the growth law can be determined to have an exponent of  $a_{III} = 0.40 \pm 0.03$ .

Summarizing this section, we find that the three MC kinetics in fact lead to very different dynamical behavior of the simulated system. These results will be analyzed and contrasted to the molecular dynamics results in the next section.

#### 4. DISCUSSIONS AND CONCLUSIONS

Summarizing the preceding two sections on molecular dynamics and Monte Carlo results, we have found qualitative agreement for the respective cluster growth patterns during the phase separation process. This is demonstrated in Fig. 1, where the snapshot pictures of the molecular dynamics simulations and of the MC simulations (version I) are compared. The neighboring pairs of figures are chosen such that the corresponding values of the mean cluster radius  $R$  agree. We also find characteristic power laws for the growth of  $R(t)$  in molecular dynamics and of  $R(\tau)$  in all versions of Monte Carlo simulations for the late-time regimes. Additionally, for molecular dynamics and MC versions I and III we obtain scaling of the cluster radial distribution function in those regimes.

These findings might lead to the impression that the overall behavior in all cases is very similar. However, a closer inspection of the obtained results reveals distinct differences. However, we want to emphasize that the



differences between the molecular dynamics results and those of the MC simulations are not only due to the different numerical procedures but also due to the different physical systems studied. Molecular dynamics simulations have been performed for a continuous system with Lennard–Jones interaction of the atoms, while Monte Carlo simulations were done for a discrete Ising system with nearest-neighbor interactions. Nevertheless, one could be led to the conclusion that these differences should not influence the long-time behavior of the spatial decomposition process. This conclusion is not supported by our findings.

A first hint of the differences may be seen in the last two pairs of snapshot pictures in our Fig. 1. In these snapshots the molecular dynamics pattern (left side) seems to consist of more isolated clusters than the MC pattern. This is not obvious from the pair correlation function; one would have to analyze higher-order correlation functions for quantitative results. The cluster pair correlation function looks very similar in both cases due to the involved spherical averaging and the fact that the individual clusters contribute proportional to their respective number of atoms, thus effectively suppressing contributions from the smaller ones.

Even the details of the spatial structure of  $g(r)$  are very similar in the molecular dynamics and MC version I simulations. However, already in the MC version II the spatial variations of  $g(r)$  are strongly reduced. This demonstrates clearly that different MC versions, which nevertheless yield the same equilibrium properties lead to different growth patterns.

We now discuss the time-dependence and the scaling of the cluster distribution function  $g(r, t)$  or  $g(r, \tau)$ , respectively. In Table I we summarize the exponents of the growth laws for  $R$  in the late-time regimes.

In molecular dynamics  $R \propto t^a$ , where  $t$  is the physical time, whereas in MC  $R \propto \tau^a$ , where  $\tau$  is the “MC time” measured in MC steps per atom.

Let us first discuss the molecular dynamics result.

Explicit theoretical calculations of the power law can be performed on the basis of a Lifschitz–Slyozov analysis<sup>(14)</sup> of the appropriate dynamical equations. This has been done in Ref. 8. However, the basic results of this analysis can be understood easily, once one knows that a power-law behavior is an adequate description.

One analyzes the dynamic equation for the growth of the mean cluster

Table I.

Simulation	Exponent $a$
MD	$0.50 \pm 0.02$
MC(I)	$0.25 \pm 0.01$
MC(II)	$0.38 \pm 0.08$
MC(III)	$0.40 \pm 0.03$

radius, which has the form

$$\frac{dR}{dt} \propto \frac{1}{R^\gamma} \left( \frac{1}{R_c} - \frac{1}{R} \right)$$

where  $R_c(t)$  is the critical cluster radius, which is essentially inversely proportional to the supersaturation in the gas phase.

If this equation is to be satisfied by an ansatz of the form

$$R \propto t^a$$

we get

$$R_c(t) \propto R(r)$$

and

$$a = 1/(\gamma + 2)$$

In the one-component system at constant temperature  $\gamma = 0$  and thus  $a = 0.5$ , and for constant energy  $\gamma = 1$  and  $a = 0.33$ ,<sup>(8)</sup> as is the case in the analysis of phase separation in binary mixtures in the original Lifshitz–Slyozov analysis.<sup>(14)</sup> Thus, the molecular dynamics results are understood to be in good agreement with theoretical predictions.

Concerning the Monte Carlo results, it is obvious from Table I that the three different versions yield different exponents  $a$ . These differences are only due to the different states available for a randomly chosen atom to be displaced. For version I, where only nearest-neighbor jumps are allowed, we have a plausibility argument supporting the value of  $a = 0.25$ . We see that at late times the clusters grow only by absorbing molecules from the gas phase, which have to be provided by the smaller clusters. Thus the effect governing the temporal behavior is the “random walk” of the monomers through the set of vacant lattice sites between the clusters. The MC time  $\tau$  to trespass the distance  $l$  between two clusters will be proportional to  $l^2$ . In the molecular dynamics simulations on the other hand, the atoms in the gas phase move linearly between the collisions, the time to travel a distance  $l$  is directly proportional to  $l$  as long as  $l$  is smaller than the mean free path in the gas phase. Elimination of  $l$  from these relations leads to  $\tau \propto t^2$ . Thus the result  $R(\tau) \propto \tau^{0.25}$  of MC version I will be consistent with  $R(t) \propto t^{0.5}$  of the molecular dynamics simulations. It is not entirely clear to us how far this agreement is only fortuitous, but nevertheless it explains why the growth law of  $R$  in the MC simulations version I is slower than that of the molecular dynamics simulations.

Two final conclusions may be obtained from the comparison of the different simulations of spinodal decomposition:

(i) In molecular dynamics the time evolution in the density pattern is uniquely determined by the physical properties of the simulated system. This is not the case in MC, when stochastic kinetics are used which only

guarantee the correct equilibrium values. To obtain reasonable dynamic results, additional restrictions must be imposed on the elementary stochastic process to mimic the true physical time-development.

(ii) Spinodal decomposition in continuous one-component systems exhibits growth rates distinctly different from two-component systems. The necessary next step for a systematic comparison would be to perform MC and molecular dynamics simulations for the same system. This would allow to extract more details about the dynamic nature of the MC simulation method.

## ACKNOWLEDGMENT

The authors thank Prof. Stauffer for the idea to write this paper. This work is project of the Sonderforschungsbereich 65 Frankfurt/Darmstadt financed by special funds of the Deutsche Forschungsgemeinschaft.

The computations have been performed on the computing facilities of the GSI, Darmstadt.

## REFERENCES

1. J. S. Langer, M. Bar-On, and H. D. Miller, *Phys. Rev. A* **11**:1417 (1975) and references therein.
2. J. W. Cahn, *Trans. Metall. Soc. AIME* **242**:166 (1968) and references therein.
3. W. I. Goldburg, in *Scattering Techniques Applied to Supramolecular and Nonequilibrium Systems*, S. H. Chen, B. Chu, and R. Nossal, eds. (Plenum Press, New York, 1981), p. 383, and references therein.
4. See, e.g., the review article of K. Binder, in *Systems Far from Equilibrium*, L. Garrida, ed. (Springer, Berlin, 1980), p. 76.
5. J. D. Gunton, M. San Miguel, and P. S. Sahni, The dynamics of first order phase transitions, preprint, 1983.
6. S. W. Koch, R. C. Desai, and F. F. Abraham, *Phys. Lett.* **89A**:231 (1982); *Phys. Rev. A* **26**:1015 (1982).
7. J. L. Lebowitz, J. Marro, and M. H. Kalos, *Acta Metallurgica* **30**:297 (1982) and the given references to the author's work partly in collaboration with other authors.
8. F. F. Abraham, S. W. Koch, and R. C. Desai, *Phys. Rev. Lett.* **49**:923 (1982); S. W. Koch, R. C. Desai, and F. F. Abraham, *Phys. Rev. A* **27**:2152 (1983).
9. See, e.g., J. Kushick and B. J. Berne, in *Statistical Mechanics Part B*, B. J. Berne (ed.) (Plenum Press, New York 1977); A. Rahman, *Phys. Rev.* **136**:A405 (1964); L. Verlet, *Phys. Rev.* **159**:98 (1967).
10. F. F. Abraham, *Phys. Rep.* **53**:95 (1979).
11. K. Binder (ed.), *Monte Carlo Methods in Statistical Physics* (Springer, New York, 1979).
12. K. Binder (ed.), in *Monte Carlo Methods in Statistical Physics* (Springer, New York, 1979), p.14; also, e.g., D. Levesque *et al.*, p. 48.
13. H. J. Leamy, G. H. Gilmer, and K. A. Jackson, *Phys. Rev. Lett.* **30**:601 (1973).
14. I. M. Lifshitz and V. V. Slyozov, *J. Phys. Chem. Solids* **19**:35 (1961).